

Review

Scheduling and realizing image-assisted robotic processes fusing adapted, minimally invasive, harmless and truthful therapies

Adel Razek

Group of Electrical Engineering—Paris (GeePs), CNRS, University of Paris-Saclay and Sorbonne University, F91190 Gif sur Yvette, France;
adel.razek@centralesupelec.fr

CITATION

Razek A. Scheduling and Realizing Image-assisted Robotic Processes Fusing Adapted, Minimally Invasive, Harmless and Truthful Therapies. *Imaging and Radiation Research*. 2026; 9(1): 026130001.
<https://doi.org/10.24294/irr026130001>
1

ARTICLE INFO

Received: 03 June 2025
Accepted: 01 April 2026
Available online: 20 April 2026

COPYRIGHT



Copyright © 2026 by author(s).
Imaging and Radiation Research is published by EnPress Publisher, LLC. This work is licensed under the Creative Commons Attribution (CC BY) license.
<https://creativecommons.org/licenses/by/4.0/>

Abstract: This contribution aims to analyze medical interventions scheduled and executed using image-guided robots. Such interventions, which can be surgical or restricted drug delivery, involve minimally invasive, precise, and harmless therapies. The accuracy of robotic positioning is trained via uncertainty and complexity reductions. This could be achieved by matching real and virtual procedures involving physical and virtual phantoms of the relevant part of the living tissues. Such tailored training includes personalized, patient and interventional tool features. The training results enable a real (with patient) intervention controlled by staff and a possible matched autonomous intervention under staff supervision. The paper includes regards on the control and monitoring of image-guided procedures, and on augmented matched digital twins for real interventions. The various topics covered in this narrative review, are supported by examples from the literature.

Keywords: image-guided therapeutics; living tissues; surgery and drug delivery interventions; complexity; uncertainties; monitoring paired real-virtual twins

1. Introduction

Throughout the history of evolution, the concentration on advancement has never ceased. Today, many routine procedures and devices typify the well-being of modern humanity. One of the most significant fields of this well-being relates to all health-linked strategies that permit safety, comfort, and healing outcomes. Recent advances in medical science have involved the discovery of the causes of many diseases and strategies to deal with their threats. These strategies mainly involve surgical and drug administration medical interventions. Traditionally, in open interventions, the abovementioned health-linked factors depend entirely on the tactile and visual skills of the medical team. These aim to be the least invasive and most accurate in terms of positioning. Thus, they protect healthy tissues contiguous to the hostile tissues involved. In addition, medical staff are supposed to practice individualized patient care, which strengthens the abilities required for operational efforts. The concept of personalized medicine comprises medical care adapted to the particular requests of each patient, considering in addition to the specific disease to be treated, factors such as hereditary features, daily life, the ecological environment and the response to treatments.

Following the above discussion, the less invasive and positional accurate tactile and visual skills could be beneficially replaced by committed image-guided robotic means [1-4] or equivalent strategies such as robotic and laparoscopic intervention [5]. In fact, a robotic intervention could be considered as the daughter of a laparoscopic one with an evident enhancement in instruments and also in the surgeon's exhaustion

who adopts a more relaxed position during the whole procedure. Such substitution is principally indorsed for more complex interventions. Moreover, such interventional complexity that can be encountered during major surgical interventions [6-9] or restricted drug administration [10-12] that requires acting in a constrained area, as mentioned before, to protect healthy living tissues neighboring the affected area. Thus, closed-loop robotic or laparoscopic processes would allow complex interventions reflecting positioning accuracy, minimally invasive (MI) and area-restricted medical decisions through assistance using means harmless to healthy living tissues [4,5]. In such closed-loop robotic control processes, different problems may be encountered, related to the administration of complexity, uncertainty and unexpected hazardous incidents. Such dilemmas can be solved by using a control strategy based on matched physical-virtual pairs [4,13]. Thus, the concept of personalized medicine as well as the abovementioned medical decisions could be predetermined by monitoring a matched real-virtual pair (involving a physical phantom and its model) allowing the verification of the intervention outcome. This supervision can be facilitated by human involvement. Moreover, in the meantime, a monitoring of the real-virtual pair could be autonomous in the presence of the patient and with the staff in the loop.

The aim of this narrative review is to analyze complex personalized medical interventions using image-guided robotics, ensuring MI and safe conditions for precise surgical or drug delivery procedures. The management of complexity and uncertainty involved in such procedures is accomplished through adapted digital twins' tools. The paper sections are summarized as follows. The second section is devoted to the contrast of traditional open and MI interventions. The third section is dedicated to image-guided medical interventions involving characteristics of adapted interventional scanners. The forth section concerns the control and monitoring of image-guided interventional procedures including closed-loop control of image-assisted robotics, and the reduction of disruptive factors in this control by monitoring real-virtual pairs, digital twins (DT). The fifth section is dedicated to the governing mathematical equations. **Section 6** is related to monitoring involvements by DT, potential staff in the loop and augmented DTs for real interventions (with patients). Finally, conclusions and future suggestions are given in the last section.

2. Open and MI interventions

Both open and MI intervention techniques are commonly practiced and have different characteristics and advantages. The open procedure is the customary method that has been expended for many years. In this case, generally one large cut is fashioned to get into the spot of the operation. This opening permits to directly see and get into the organ tissue being worked on. The open technique permits some profitable situations, as distinct sight of the interventional zone, letting accurate handling and skill, and enhanced access to intricate or outsized configurations that might be challenging to attain in MI practices. Conversely, open intervention presents a number of weaknesses. The big cut can steer to further suffering, superior bleeding, and an elongated healing interval. Moreover, there is a greater threat of infectivity and a big cut trace.

The two commonly used MI procedures are laparoscopy and computerized

robotics. Laparoscopic intervention uses some slight cuts on body surface, in the range of cm. Across these tiny openings, dedicated interventional mechanisms and a miniature camera named laparoscope are introduced. This technology evolves, different benefits related to MI incisions and increased laparoscope vision of the process zone. They respectively help reduce pain, bleeding, healing period and noticeable scars, as well as precise and manageable engagements. Laparoscopy is very commonly used in abdominal surgeries and also as diagnostic tool [14]. Conversely, laparoscopy procedure might be incompatible with all cases concerning patients or intervention types [15] and needs in general devoted training and instrumentation. Actually, intricate procedures such as neurosurgery might yet necessitate open technique or more sophisticated robot-assisted laparoscopic techniques [16]. Note that the difference between laparoscopy and its robotized option relates mainly to the medical staff's state of affairs, regarding surgical dexterity, ergonomics and ease of execution. When it comes to robotic intervention, the goal is generally not to take the place of the surgeon but to increase his ability to care for the patient. The robot is therefore a surgical device that is managed by a computer, where its control is commonly shared between the surgeon and the computer. Medical robots are therefore often referred to as surgical aides [17]. Surgical robots involve different practices or prospective categories depending on their concept and corresponding appropriate types of intervention [18].

3. Image-guided interventions

As mentioned earlier, the adoption of an interventional approach depends on different factors, including the illness, the procedure complexity and the staff expertise. Only once a complete valuation can the most fitting selection be presented to the patient, evidence-based verdict making [19]. MI techniques permit further duties to be executed with enhanced dexterity, ergonomics, and staff facility. A cutting-edge expanded approach of such practices, going further regarding task augmentation, could be image-guided robotic involvement, thus using the robotic positioning precision and 3-D high-resolution vision owing to scanner imaging. In effect, seeing only vision and positioning abilities, only image-guided procedure practices instantaneous imaging, helping in prompt locating.

The image-guided robotic MI interventions generally increase patient comfort and safety, accompanied by execution precision and successful therapeutic outcomes. Moreover, such methodologies can work at almost all body areas, involving surgery or embedded restricted drug release. Even though the imaging means are specially made for each to explicit circumstances [20], those engaging ionizing radiations as positrons or X-rays, look inapt for cures of wide duration, as in the situation of image-guided procedures. Thus, scanners matching such lengthened jobs are those displaying nonionizing features, precisely ultrasound and magnetic resonance [21]. This avoids the potential harmful effects of ionizing radiation on the living tissues involved and the surrounding healthy tissues. A scanner is assumed to dispense a 3-D high-resolution view of tissue specimens together with the involved robotic tools. Thus, the scanner abilities and the robot competencies are merged in a talented task. These two nonionizing scanners can accomplish the aforesaid burden with particular limitations

for each. The ultrasound can only be executed in airless and boneless frames [3,4] while MRI entails a scaffold environment free of electromagnetic field (EMF) [22] but can operate universally in all body organs. It should be noted that ultrasound has suitable malleability and cost, while MRI, which permits exceptional soft tissue images, is more expensive and has a more intricate use. Choosing between the two scanners thus depends on the situation. However, once patient comfort and safety are imperative, such as in brain interventions, the use of an MRI-guided procedure becomes compulsory.

4. Control and monitoring of MRI-guided plans

Image-guided interventions that adopt security require linking to scanners and clinical procedures generally exploit MRI and ultrasound imaging [3,4,23]. MRI scanners are progressively being used in interventions, mainly owing to their higher skill to discriminate tumors from healthy tissue in events involving tumor extraction [24]. As aforesaid, an MRI scanner is EM-sensitive and could be troubled by external EMFs as well as the introduction of external substances; thus, robotic constituents hosted in its scaffold must be MRI-compatible, i.e., devoid of magnetic or conductive ingredients. However, robotic arrangements normally necessitate high-performing actuation dealings, while a small number of actuator categories perform in an MRI-compatible mode. One possible group of actuation tools that are usually MRI-compatible utilizes piezoelectric constituents, which come in diverse brands. More details about their configurations, manufacture, investigation, and usages are presented, for example, in [25-27]. These tools are free of magnetic stuff and fashioned of dielectric piezoelectric ingredients, but provided with tinny and non-massive conductive electrodes required for their excitation. Indeed, piezoelectric materials are known to be compatible with MRI, while the compatibility of electrodes despite their size poverty depends on their material characteristics and organizational structure and therefore requires validation as a precaution.

4.1. Closed-loop control actions

The consistency of tissue zone restriction is linked to the actuation accuracy of the medical tool and its positioning in the working area. Consequently, the necessity for such superior area tracking suggests an image-coordinated position identification. This entails a cooperative arrangement running independently, as shown by the representation of a self-controlled surgical background in **Figure 1**, including scanner, tissue-touched zone, surgical tool, position and actions processing, robotic control and actuation [3,4]. The accuracy implicated in such a closed-loop control process, associated with location positioning and actuation feature, would be fashioned by the amount of intricacy of the joint components of the process, the concomitant uncertainties, and different unforeseen exterior hazards. Only the reduction of such disturbing characteristics authorizes a reliable control.

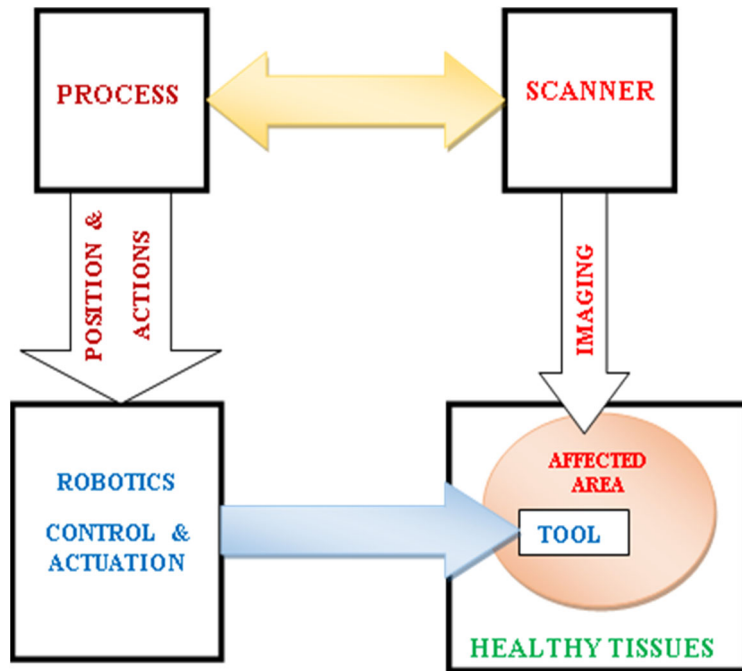


Figure 1. Schematics of a self-controlled image-guided robotic interventional procedure.

4.2. Compatibility and disturbances control

This section aims to investigate the reduction of disturbing features related to MRI compatibility, as well as image-assisted procedure complexity and uncertainty.

4.2.1. MRI compatibility

The following assessment aims to tackle the problem of MRI-compatibility of introduced stuffs linked to robotic instruments in the scanner scaffold. Such compatibility is concomitant with image faithfulness and exactness. An MRI-compatible substance is presumed not to alter the image quality. An image produced in an MRI scanner is fashioned by signals initiated by the interaction of fields with living tissues. Actually, three dissimilar fields are utilized to build 3-D images. A large static field produces a magnetization vector in tissues, bringing their protons and measuring their strength. Three little-frequency repetitive gradient fields space-locating ranged tissues protons forming a 3-D spatial reconstruction. Finally, a radiofrequency (RF) field excites the vector of magnetization in tissues, allowing its disclosure by the scanner, which can be treated and transformed into images [3].

In fact, MRI deals with the atomic nuclei of hydrogen that are enclosed inside the body. A nucleus of hydrogen is a proton that is a mass of positive charge revolving around an axis. Protons are randomly orientated in tissues, and individually spin, thus acting out of phase and exhibiting zero magnetic field. Bearing in mind the MRI theory, protons in tissues entail three engagements: aligning protons in an established direction, rotating them together, and localizing their distinct place of origin. Such organization could be respectively accomplished by: a static field B_0 , a RF field B_1 pulsating with the natural frequency of protons' rotation f_L (Larmor frequency) permitting a resonance action, and 3-D space gradient $G(x, y, z)$ operated to the field

B_0 , allowing distinct position values of $B_{0d}(x, y, z) = B_0 + G(x, y, z)$. The value of f_L is B_0 dependent and equal to 42.5 MHz per tesla, and the conforming distinct position values $f_{Ld}(x, y, z)$ are $B_{0d}(x, y, z)$ dependent. As abovementioned the three MRI operated fields, contrast in strength, frequency and presence. Thus, B_0 : 0.2–10 T, 0 Hz, always present; gradient: 0–50 mT/m, 0–10 kHz, pulses of a few ms; B_1 : 0–50 μ T, 8–300 MHz, (amp. mod. pulses) of a few ms. An illustration of the MRI field components is shown in **Figure 2**.

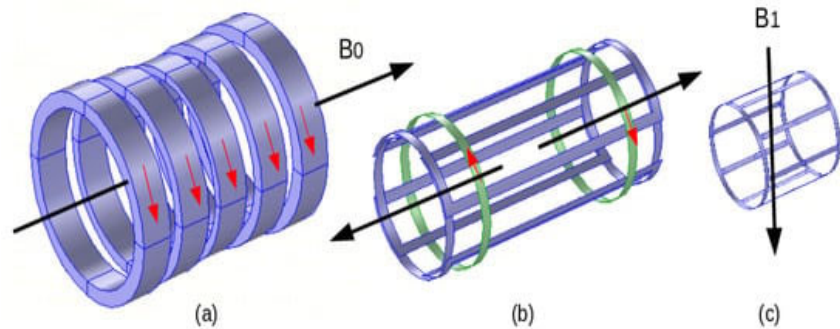


Figure 2. MRI fields: (a) electromagnet B_0 , (b) gradient coils (one couple for one axis), (c) RF coil (birdcage) B_1 .

The components generating the MRI involved fields are generally protected. The static and gradient fields are compensated and regulated. The RF field coil (frequently birdcage form, **Figure 2c**) that is basically related to the image, is the most unprotected against worries principally due to introduced external substances in the MRI scaffold. Thus, the MRI-compatibility of an object inserted in the scaffold, inside the birdcage, is controlled through its impact on the field distribution of B_1 , i.e., for an MRI-compatible object, the field distributions with or without the object are identical. Thus, the compatibility could be verified through computations of the field distribution in the birdcage of B_1 .

4.2.2. Complexity and uncertainty treatments

As stated previously, the accuracy concerned in the image-assisted robotic control related to actuation and frame positioning is dependent on disturbing dynamics, containing the complexity amount of diverse implicated combined constituents, the allied detection uncertainties, and uncommon external hazard happenings. The suppression of such possible distresses, besides the concern of particular distinct process data, is necessary for the truthful running of the controlled image-guided practice. Such purposes could be accomplished by monitoring the concerned factors in a corresponding real-virtual pair through a digital twin (DT) implementation [28]. A DT is typified by the incorporation of information within a couple of a physical occurrence and its digital replica, paired in a two-way conduct. Such methodology is experienced for management of complexity in regulated processes [29] and arranged as a physical-virtual pair permitting self-adapting behavior. Thus, the physical wing of the pair distributes processed detected data to the virtual wing, while the latter conveys control instructions to the physical wing. These matching supports reducing pair uncertainties and unforeseen irregularities in procedure control. It thus seems obvious that the supervision of complexity,

uncertainties and irregularity by DT answers well to the disturbing dynamics of image-assisted robotic control stated above. Newly, DT has been increasingly established in the health area, facilitating associated nursing and continued administration of disturbances. Many circumstances have been considered for this goal, see e.g., [30-33].

4.3. DT supervision of MRI-assisted interventions

The specified DT supervision arrangement of an image-guided robotic procedure is described in this section. Generally, regarding the abovementioned exchanges between the DT wings, the processed information of the real wing distributes sensed data matched and corrected, by peripheral “IoT” information and acquired historical data. The achieved result, once experienced as data analysis, is transferred, with a suitable reduced model suggestion, to the virtual wing. In fact, a swift interaction (corresponding) between wings of DT requires an accurate virtual replica but with little finishing time. Thus, the all-inclusive coupled model, which truthfully signifies the real procedure, would be condensed, permitting weak calculation time but conserving the essence of the actual process. Supervision of an image-guided robotic control using an amended DT implementation achieves an effective adaptive control process linking the actual process paired with a reduced model [34]. **Figure 3** shows the structure of such a process. Such supervising could be exploited for personnel training, forecasts using bodily phantoms and their digital copies, or an actual patient–virtual duplicate model, containing self-governing corresponding with personnel in the loop.

The implicated coupled model comprises wholly constituents and deeds of the image-piloted robotic procedure shown in **Figure 1**. As mentioned, the two MRI magnetic fields of the static and gradient fields are compensated and adjusted. Also, the RF field distribution is correlated to the images. This arises through the treatment and conversion of the signals succeeding the excitation and restoration of the B_1 -wave. Therefore, the 3-D distribution of the RF field in the birdcage containing the tissues and the robotic tool that stands for the result of the imaging procedure, can be used for the control of the MRI-compatibility of the tool.

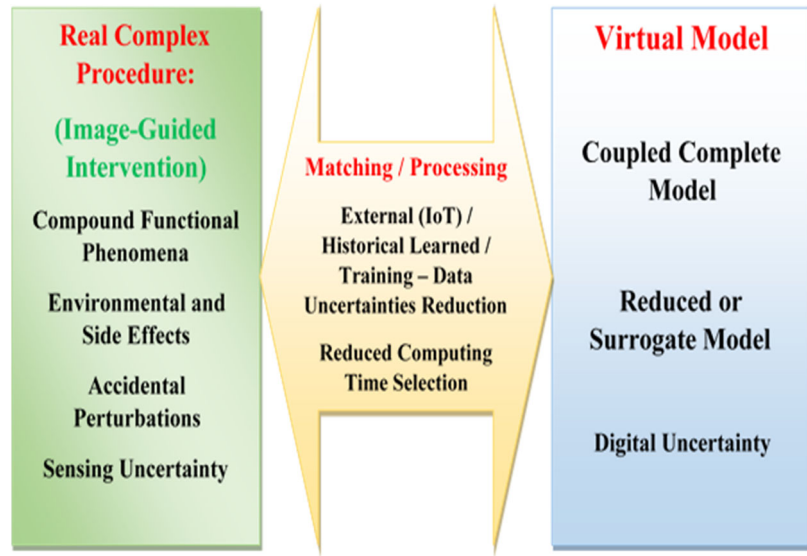


Figure 3. Schematic demonstration of the attributes of a DT monitoring an image-guided robotic intervention.

5. MRI RF field governing equations

As aforementioned, the restoration of the RF wave in the MRI scaffold yields a 3-D field distribution allowing the following signal treatment and image transformation to attain a 3-D image of tissue specifics together with a robotic tool. The mathematical governing equations of such RF field occurrence are founded on Maxwell's local behavior differential shape of the universal EMF equations [35]. In the circumstances of RF EMF radiation of living tissues, we can expand the subsequent harmonic formulation of EMF:

$$\nabla \times \mathbf{H} = \mathbf{J} \quad (1)$$

$$\mathbf{J} = \mathbf{J}_e + \sigma \mathbf{E} + j \omega \mathbf{D} \quad (2)$$

$$\mathbf{E} = -\nabla V - j \omega \mathbf{A} \quad (3)$$

$$\mathbf{B} = \nabla \times \mathbf{A} \quad \text{with } \nabla \cdot \mathbf{A} = 0 \quad (4)$$

In Equations (1–4), \mathbf{H} and \mathbf{E} are the vectors of the magnetic and electric fields in A/m and V/m, \mathbf{B} and \mathbf{D} are the vectors of the magnetic and electric inductions in T and C/m², \mathbf{A} and V are the magnetic vector and electric scalar potentials in Wb/m and volt. \mathbf{J} and \mathbf{J}_e are the vectors of the total and source current densities in A/m², σ is the electric conductivity in S/m, and ω is the angular frequency = $2\pi f$, f is the frequency in Hz of the exciting EMF. The symbol ∇ is a vector of partial derivative operators. The magnetic and electric compartment laws, respectively, between \mathbf{B}/\mathbf{H} and \mathbf{D}/\mathbf{E} are represented by the permeability μ and the permittivity ε in H/m and F/m.

The solution of these equations must consider specific characteristics of the concerned constituents, such as geometrical intricacy, material inhomogeneity, variables nonlinearity, which suggest sophisticated computational methodologies. Satisfying such features inflicts material local response implying the use of discretized 3-D approaches, such as the finite element method (FEM) or similar methods as BEM,

FDTD, etc., [36-39]. The solution might be expanded to attest the MRI-compatibility of the diverse stuff hosted in the MRI scaffold, by means of EM compatibility (EMC) practices [3].

5.1. DT virtual models

The DT process supervising tool (**Figure 3**) comprises a process-coupled model [40] and its condensed or surrogate form [41,42]. Virtual arithmetical models (numerical phantoms) can typify the body part living tissue implicated in the intervention. Significant characteristics of such models should match the nature of the substance and biological properties, structural form and reliability of the used computational methodology. Diverse body replicas with living tissue features could be found in the literature [43-45].

5.2. EMC MRI-compatibility analysis

The MRI scanner shows sensitive reactions to EM interference due to exposure to peripheral EMFs or enclosure of EM-sensitive ingredients into the scaffold, both of which can disturb the scanner's own EMFs. The MRI EM-sensitive substances are mostly ferromagnetic and conductive constituents. Bearing in mind that the static and gradient fields are balanced and controlled as mentioned formerly, the interaction of a matter hosted in the scaffold with the RF B_1 wave can be analyzed. With such an analysis, the matter's compatibility with MRI can be validated or established. Thus, the EMC analysis permits the detection of the influence of the enclosure of outside ingredients into the MRI scaffold on the 3-D B_1 field distribution, which is image correlated, acquired from the solution of (1-4). These equations are solved for a specified field excitation size and frequency alongside the behavior laws parameters σ , μ , and ϵ of the introduced stuff.

As aforesaid, typical MRI-compatible robotic piezoelectric actuators are furnished with thin electrodes required for their excitation. These conductive electrodes could be accountable for the trouble of the 3-D RF B_1 field distribution, owing to their eddy currents provoked by this field. These currents principally hang on the perpendicular conductive surface to the field. Such an incident might be utilized in the actuation to reduce disturbance in the MRI RF field distribution [4]. Perturbation check could be accomplished by corresponding the field distributions with and without the hosted object. **Figure 4** displays the RF field B_1 distribution (vertically directed) in the cross-section of an unoccupied birdcage inside the scanner tunnel. **Figure 5** shows an instance of a cubic piezoelectric coated by thin electrodes on two opposed sides of the cube, exemplifying a simple piezoelectric actuator (**Figure 5a**). **Figure 5b,c** exhibit the field distributions in the two circumstances with the electrodes respectively perpendicular and parallel to the field.

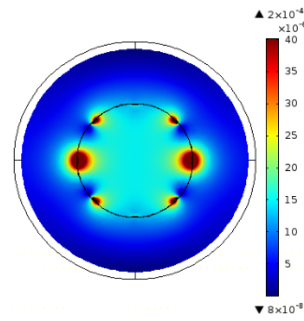


Figure 4. MRI RF B_1 —vertically directed—(at 63.87 MHz, B_0 1.5 T) distribution in the situation of no material [4].

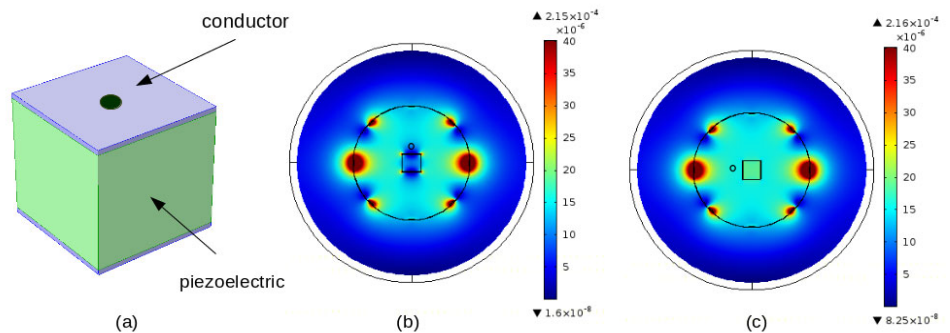


Figure 5. MRI RF B_1 (vertically directed) field distribution in the case of insertion of a piezoelectric covered by two electrodes, (a) material framework (b) distribution of B_1 field—electrodes perpendicular to the field (c) distribution of B_1 field—electrodes parallel to the field [4].

It should be noted that the conductors' influence, in the situation (parallel to the field), is radically diminished (**Figures 4 and 5c** are almost the same). These outcomes demonstrate a simple qualitative instance of likely EMF interference image perturbation and hence actuation potential by dropping such disturbance.

6. DT monitoring concerns

6.1. Projecting of medical plans

The DT administration of the MRI-guided procedure needs preparation to fine-tune and validate the different medical schedules. This would be achieved by means of material phantoms and their digital models in the DT implementation. These pre-appointments comprise patient and interventional specified data, conforming to adjusting scanner parameters, MRI compatibility of articles enclosed in the scaffold, and associated actuation and handling of robotics concerns of the involved intervention.

6.2. Implementation and training prospects

The preparation stated in the previous section permits the easy management of the commitment and the projected corrections involved in the therapeutic process. Thus, the forthcoming intervention comprising the patient might be achieved in a straight imaging-assisted cooperative environment, under personnel administration, or

conceivably as an autonomous DT monitoring procedure including medical staff in the loop. Furthermore, such tuition authorizes staff to predict the disorders that patients may possibly endure within the intervention. Such disturbances could be connected to robotic medical tools, operations or drugs. Additionally, the DT patient individualized scheduling task allows the medical team, in a risk-free way, deprived of patient, to execute processes, adjudicate judgments, and be conscious of possible assessment errors [4,46].

Concerning living tissues of diverse body portions, they are signified in the DT on two sides, by material phantoms and their digital copies. The tissue conducts in these phantoms (physical and digital) are of a static nature, which could be satisfactory for some organs in the situation of particular processes. Nevertheless, these representations are presumed to allow for real tissues' biological conduct [47]. The genuine soft tissues' behavior relates to an intricate, lively dynamic conduct matching the displacement and deformation mechanics of living soft tissues [48,49].

6.2.1. Human participation and augmented DT

Human-robotic alliance surfaced by the DT concept with staff in the loop permits sophisticated image-guided administration of medical interventions, thus decreasing the patient menace and guaranteeing a consistent finish for the staff [50]. Furthermore, artificial intelligence (AI) practices in such treatments aid in lessening the intricacy of data acquisition and post-processing and in achieving repeated scheduled training tasks [51]. Additionally, the involvement can be considerably enhanced across magnified human-robot links, developing the whole organization by means of augmented reality (AR)—guided robotic deeds. Consequently, AR joint to MRI scanner can reduce hazards in complex clinical dealings, such as tissue injury, bleeding, and post-interventional distress. As well, DTs can accomplish a significant duty in AR-assisted robotic involvement. Therefore, the probable disturbance source and its remedying could be precisely detected via personal patient analysis owing to deep learning databanks. Likewise, several added profits of mutual AR-DT are possible regarding enhanced correctness in suturing, sticking, and fixation paralleled to manual duties [50,51].

6.2.2. Potentials of tutoring

DT can potentially renovate patient healthcare by gradually conveying individualized and data-driven therapeutic attention. Its practice is share of digital care and is generally exploited in personalized therapeutic cures, which allow malady observing and detection, tutoring, or interventions. DTs are frequently allied, as mentioned above, to AI and AR tools, besides virtual reality (VR). Equally, VR tuition advances the capacity to reproduce routine training conditions with the facility to correctly gauge execution. Tutoring principally comprises scheduling an individualized session or investigating new dealings as part of overall training.

The necessary DT tuition of starting personnel is linked to the founding of virtual body and anatomy representations to allow execution, proficiency amplifying, and perfecting their insight into the body issues. DT regular staff training includes carrying out scenarios, fulfilling essential characters, administering drugs, and facing critical conditions. This can be linked to patient attentions, e.g., cardiac incidents, or environmental conditions, e.g., fires. Moreover, DT permits tutoring in the usage and

care of therapeutic tools and infection control processes. Additionally, training of DTs permits personnel to watch the evolution of disorders and adjust treatment strategies, choosing the most appropriate therapy. Such tutoring in personalized scheduling aids to progress early judgment and investigate new handling or interventions [52].

7. Discussion

The outcomes of this review emphasized the significance of MI, non-ionizing, and accurate interventions. In addition, acquiring the benefit of a suitable digital environment permits staff to plan, forecast, search, tutor, and execute with staff in the loop. Following the above analyses, several questions merit more discussions:

The chronological classification of interventional strategies is often related to procedural innovations such as optical fibers, robotics, numerical control, DT, etc., and mainly to their use in medicine (see e.g. the studies of [3,53]). This contribution, in addition, has underlined some capacities proposed by the choice of image-assisted interventions and by DT monitoring of their controlled procedure.

Concerning the procedural innovations cited in the preceding point, these are frequently given as pioneering due to their use in modern attention, even if their idea existed earlier, such as the link between neural networks and AI. Same as the recent concept of DT introduced by Grieves in 2002 [29], which practices a similar strategy to the oldest survival tactic, namely, camouflage styled by Bates in 1862 [54], which permits creatures to merge into their surroundings, thus hiding owing to adaptive matching.

In the above examination of DT supervising (tracking), the considerations of complexity, swift matching, coupled and reduced models have been tackled at different places. In effect, these concepts are interrelated. An accurate correspondence of a physical complex process with its virtual model infers the use of a complete coupled model [55]. The problem with this last is its enormous execution time, incompatible with quick simultaneous matching. Therefore, the complete model should be reduced without damaging its precision [56]. Attaining the limit between swiftness and failing truth, a surrogate model could therefore be substituted [57,58] for the complete model or one can implement non-intrusive stochastic methods, such as kriging and polynomial chaos [59,60], advancing helpful Meta models.

The three different MRI fields B_0 , B_1 , and G are supposed to be safeguarded and safe for patients and medical staff when using scanners with modest efficacy (static field asset and gradient output). For lately great-performing scanners, some distressing worries could be perceived and the scanner's involved fields can trigger uncomfortable consequences for patients or adjacent staff. These concerns mainly involve the pulsed gradient G and the static B_0 fields, due to the high output (strength and scanning swiftness) of the first and the ultra-high-field (UHF) above 7 T in the second in recent high-performance scanners. Indeed, high output G , which permits smaller imaging duration, can produce peripheral nerve stimulation (PNS) [61,62] and the UHF B_0 [63] can induce currents and hence fields in body tissues moving inside or near the scanner [64], triggering different painful feelings. Moreover, such interaction of B_0 with moving body fashions magnetic induction effects associated with induced currents and Lorenz forces [65], depending on the movement speed and the field strength and hence

in case of UHF, different disturbances could happen, e.g., magnetic vestibular stimulation (MVS) [66]. Other common side effects of these forces could be found in [67,68].

Regarding the accuracy of robotic positioning and its repeatability, a robot's correctness is its ability to attain a particular target in its workspace. It certifies that it can track planned orders to execute duties calling for accurate locating. Precision hang on sensors, control scheme, and environmental circumstances. Robotic consistency is associated with repeatability, which rates how consistently it goes back to the same position. It is shaped by joint constancy (a measure of actuation drift), adjustment, and robustness [69].

Disturbances in MRI-assisted robotic involvements could be reciprocated. Thus, the MRI scanner is allergic to EM interference triggered by robotic concerns, and the robotic control scheme may also be traumatized by the scanner's fields [70].

MRI-compatible robotic instruments could involve, as mentioned in the above analysis, piezoelectric actuators that reflect a relatively small intrinsic motion range. Actually, the range can be expanded by an exterior process of mechanical movement enlargement, straight or obliquely, by transforming deformation into movement. The oblique expansion uses generally sophisticated structures, recurrence, and/or striding approaches. Thus, enlarged actuators can accomplish longer strokes and higher degrees of freedom [71].

Regarding the challenges of DT monitoring, particularly in the areas of health and human participation DT (see **Section 6**), several recent studies are available in the literature, for example [72-75]. Recent articles [76-78] relating to intelligent digital management and robotic actuation of interventions can also be quoted.

8. Conclusion

The proposed contribution participated in the analysis of complex medical interventions involving an image-assisted robotic process under MI, non-ionizing and precise surgical or drug delivery conditions. Scanners suitable for robotic interventions, control and monitoring, as well as mastering their disruptive factors and planning of personalized and medical decisions with augmented prospective routines, were analyzed and discussed. As a conclusion of this study, digital twins already integrated in healthcare could provide, combined with digital tools, an effective solution for the management of image-assisted robotics. This could be implemented in different forms, including training, planning and control interventions through the use of phantoms or involving patients with staff in the loop. A suggested future open question could be related to a deeper reflection on the mechanical behaviors of living tissues in real time.

Conflict of interest: The authors declare no conflict of interest.

References

1. Chinzei K, Hata N, Jolesz FA, Kikinis R. Surgical assist robot for the active navigation in the intraoperative MRI, Hardware design issues. Proceedings of the IEEE/RSJ International Conference on Intelligent Robots and Systems (IROS 2000), Takamatsu, Japan, 2000; 1, 727–732.

2. Tsekos NV, Khanicheh A, Christoforou E, et al. Magnetic Resonance–Compatible Robotic and Mechatronics Systems for Image-Guided Interventions and Rehabilitation: A Review Study. *Annual Review of Biomedical Engineering*. 2007; 9(1): 351-387. doi: 10.1146/annurev.bioeng.9.121806.160642
3. Razek A. From Open, Laparoscopic, or Computerized Surgical Interventions to the Prospects of Image-Guided Involvement. *Applied Science*. 2025; 15, 4826. <https://doi.org/10.3390/app15094826>
4. Razek A, Image-guided surgical and pharmacotherapeutic routines as part of diligent medical treatment. *Applied Science*. 2023; 13, 13039.
5. Marrelli D, Piccioni SA, Carbone L, et al. Posterior and Para-Aortic (D2plus) Lymphadenectomy after Neoadjuvant/Conversion Therapy for Locally Advanced/Oligometastatic Gastric Cancers. 2024; 16(7), 1376.
6. Faoro G, Maglio S, Pane S, et al. An Artificial Intelligence-Aided Robotic Platform for Ultrasound-Guided Transcarotid Revascularization. *IEEE Robotics and Automation Letters*. 2023; 8(4): 2349-2356. doi: 10.1109/lra.2023.3251844
7. Balasubramanyam A, Manwani R, Kalyanpur D, Basavaraju PB, Padmaraju SV, Honnavalli PB. A cardiovascular modeling framework for enabling personalized healthcare: A Digital Twin Approach. In 2025 IEEE 13th International Conference on Healthcare Informatics (ICHI) 2025 Jun 18 (pp. 478-489). IEEE.
8. Padhan J, Tsekos N, Al-Ansari A, et al. Dynamic Guidance Virtual Fixtures for Guiding Robotic Interventions, Intraoperative MRI-guided Transapical Cardiac Intervention Paradigm. *Proceedings of the 2022 IEEE (BIBE)*, Taichung, Taiwan, 2022; 265–270.
9. Singh S, Torrealdea F, Bandula S. MR Imaging–Guided Intervention: Evaluation of MR Conditional Biopsy and Ablation Needle Tip Artifacts at 3T Using a Balanced Fast Field Echo Sequence. *Journal of Vascular and Interventional Radiology*. 2021; 32(7): 1068-1074.e1. doi: 10.1016/j.jvir.2021.03.536
10. Xu L, Pacia CP, Gong Y, et al. Characterization of the Targeting Accuracy of a Neuronavigation-Guided Transcranial FUS System In Vitro, In Vivo, and In Silico. *IEEE Transactions on Biomedical Engineering*. 2023; 70(5): 1528-1538. doi: 10.1109/tbme.2022.3221887
11. Navarro-Becerra JA, Borden MA, Targeted Microbubbles for Drug, Gene, and Cell Delivery in Therapy and Immunotherapy. *Pharmaceutics*. 2023; 15(6), 1625.
12. Delaney LJ, Isguven S, Eisenbrey JR, et al. Making waves: how ultrasound-targeted drug delivery is changing pharmaceutical approaches. *Materials Advances*. 2022; 3(7): 3023-3040. doi: 10.1039/d1ma01197a
13. Razek A, Augmented therapeutic tutoring in diligent image-assisted robotic interventions. *AIMS Medical Science* 2024; 11(2), 210-219.
14. Bizzarri N, Pedone Anchora L, Teodorico E, et al. The role of diagnostic laparoscopy in locally advanced cervical cancer staging. *European Journal of Surgical Oncology* 2024; 50(12), 108645.
15. Li SY, Ye-Wang, Cheng-Xin, et al. Correction to: Laparoscopic surgery is associated with increased risk of postoperative peritoneal metastases in T4 colon cancer: a propensity score analysis. *International Journal of Colorectal Disease*. 2025; 40(1). doi: 10.1007/s00384-025-04810-3
16. Taghavi K, Glenisson M, Loiselet K, et al. Robot-assisted laparoscopic adrenalectomy: Extended application in children. *European Journal of Surgical Oncology* 2024; 50(12), 108627.
17. Taylor RH, Mencias A, Fichtinger G, Fiorini P, Dario P. *Medical Robotics and Computer-Integrated Surgery*. Springer Handbook of Robotics B. Siciliano and O. Khatib, Eds. in Springer Handbooks, Cham: Springer International Publishing 2016; 1657–1684.
18. Wan Q, Shi Y, Xiao X, et al. Review of Human–Robot Collaboration in Robotic Surgery. *Advanced Intelligent Systems*. 2024; 7(2). doi: 10.1002/aisy.202400319
19. Burns PB, Rohrich RJ, Chung KC. The levels of evidence and their role in evidence-based medicine. *Plastic and Reconstructive Surgery*. 2011; 128(1), 305-310.
20. Zhang B, Liu L, Meng D, et al. Medical imaging technology: Principles and systems. *INNOSC Theranostics and Pharmacological Sciences*. 2024; 7(3): 3360. doi: 10.36922/itps.3360
21. Kraus MS, Coblentz AC, Deshpande VS, et al. State-of-the-art magnetic resonance imaging sequences for pediatric body imaging. *Pediatric Radiology*. 2022; 53(7): 1285-1299. doi: 10.1007/s00247-022-05528-y
22. Haskell MW, Nielsen JF, Noll DC. Off-resonance artifact correction for MRI: A review. *NMR in Biomedicine*. 2023; 36, e4867.

23. Su H, Kwok KW, Cleary K, et al. State of the art and future opportunities in MRI-guided robot-assisted surgery and interventions. *Proc IEEE Inst Electr Electron Eng.* 2022; 110, 968-992.
24. Bernardes MC, Moreira P, Lezcano D, et al. In Vivo Feasibility Study: Evaluating Autonomous Data-Driven Robotic Needle Trajectory Correction in MRI-Guided Transperineal Procedures. *IEEE Robotics and Automation Letters* 2024; 9(10), 8975–8982.
25. Mohith S, Upadhyaya AR, Navin KP, Kulkarni SM, Rao M. Recent trends in piezoelectric actuators for precision motion and their applications: A review. *Smart Materials and Structures.* 2020; 30, 013002.
26. Wang S, Zhou S, Zhang X, et al. Bionic stepping motors driven by piezoelectric materials. *Journal of Bionic Engineering.* 2023;20:858-872.
27. Zhang S, Liu Y, Deng J, et al. Piezo robotic hand for motion manipulation from micro to macro. *Nature Communication.* 2023; 14, 500.
28. Tao F, Sui F, Liu A, et al. Digital twin-driven product design framework. *International Journal of Production Research.* 2019; 57, 3935-3953.
29. Grieves M, Vickers J. Digital twin: Mitigating unpredictable, undesirable emergent behavior in complex systems. *Trans-disciplinary Perspectives on Complex Syst.* Cham, Switzerland: Springer 2017; 85-113.
30. Sun T, He X, Li Z. Digital twin in healthcare: Recent updates and challenges. *Digit Health* 2023; 9, 20552076221149651.
31. Al-Jaroodi J, Mohamed N. Enhancing the Efficiency of Healthcare Facilities Management with Digital Twins. *International Conference on Smart Applications, Communications and Networking (SmartNets), Harrisonburg, VA, USA, 2024; 1-5.*
32. Ricci A, Croatti A, Montagna S. Pervasive and connected digital twins-a vision for digital health. *IEEE Internet Computing.* 2022; 26, 26-32.
33. Wickramasinghe N, Ulapane N, Sloane EB, Gehlot V. Digital Twins for More Precise and Personalized Treatment. In: *MEDINFO 2023—The Future Is Accessible.* IOS Press; 2024; 310, 229-233.
34. Fuller A, Fan Z, Day C, Barlow C. Digital Twin: Enabling Technologies, Challenges and Open Research. *IEEE Access.* 2020; 8, 108952-108971. doi: 10.1109/ACCESS.2020.2998358.
35. Maxwell JC. VIII. A dynamical theory of the electromagnetic field. *Philosophical Transactions of Royal Society.* 1865; 155, 459–512.
36. Henrotte F, Geuzaine C. Electromagnetic forces and their finite element computation. *International Journal of Numerical Modelling.* 2024; 37(5), e3290.
37. Gürbüz IT, Martin F, Rasilo P, Billah MM, Belahcen A. A new methodology for incorporating the cutting deterioration of electrical sheets into electromagnetic finite-element simulation. *Journal of Magnetism and Magnetic Materials.* 2024; 593, 171843...
38. Urdaneta-Calzadilla A, Chadebec O, Galopin N, et al. Modeling of Magnetolectric Effects in Composite Structures by FEM–BEM Coupling. *IEEE Transactions on Magnetics.* 2023; 59(5), 1-4, 7000604.
39. Antunes O.J, Bastos J.P.A, Sadowski N, et al. Using hierarchic interpolation with mortar element method for electrical machines analysis. *IEEE Transactions on Magnetics.* 2005; 41, 1472–1475.
40. Gu B, Li H, Li B. An internal ballistic model of electromagnetic railgun based on PFN coupled with multi-physical field and experimental validation, *Defence Technology.* 2024; 32, 254-261.
41. Kudela J, Matousek R. Recent advances and applications of surrogate models for finite element method computations: A review. *Soft computing.* 2022; 26, 13709-13733.
42. Cheng M, Zhao X, Dhimish M, Qiu W, Niu S. A Review of Data-driven Surrogate Models for Design Optimization of Electric Motors. *IEEE Trans. on Transportation Electrification.* 2024; 10(4), 8413-84311.
43. Hasgall, PA, Di Gennaro F, Baumgartner C, et al. iT'S Database for thermal and electromagnetic parameters of biological tissues 2022. Version 4.1. <https://doi.org/10.13099/vip21000-04-1> » IT'IS Foundation
44. Makarov SN, Noetscher GM, Yanamadala J, et al. Virtual Human Models for Electromagnetic Studies and Their Applications. *Reviews in Biomedical Engineering.* 2017; 10, 95–121.
45. Harris L.R, Zhadobov M, Chahat N, Sauleau R. Electromagnetic dosimetry for adult and child models within a car: Multi-exposure scenarios. *International Journal of Microwave and Wireless Technologies.* 2011; 3, 707–715.
46. Cellina M, Cè M, Ali M, et al. Digital Twins: The New Frontier for Personalized Medicine? *Applied Science.* 2023; 13, 7940.

47. Kangasmaa O, Laakso I, Schmid G. Estimating Human Fat and Muscle Conductivity From 100 Hz to 1 MHz Using Measurements and Modelling. *Bioelectromagnetics*. 2025; 46, e22541.
48. Kallin S. Deformation of Human Soft Tissues: Experimental and numerical aspects. Licentiate Thesis, Jönköping University, 2019. Available from: <https://docslib.org/doc/4193507/deformation-of-human-soft-tissues-experimental-and-numerical-aspects> [Last accessed on 17 April 2026].
49. Fung YC. *Biomechanics: Mechanical Properties of Living Tissues*. 2nd ed. Berlin: Springer-Verlag, 1993.
50. Song Y. Human digital twin, the development and impact on design. *Journal of Computing and Information Science in Engineering*. 2023; 23, 060819.
51. Katsoulakis E, Wang Q, Wu H, et al. Digital twins for health: a scoping review. *npj Digital Medicine*. 2024; 7, 77.
52. Armeni P, Polat I, De Rossi LM, Diaferia L, Meregalli S, Gatti A. Digital twins in healthcare: is it the beginning of a new era of evidence-based medicine? A critical review. *Journal of Personalized Medicine*. 2022; 12, 1255.
53. You C, Lu H, Zhao J, Qin B, Liu W. The Comparison Between Traditional Versus 3D Printing Combined with Computer Navigation Technique in the Management of Orbital Blowout Fractures. *Journal of Craniofacial Surgery*. 2025; 36, 201–205.
54. Bates H.W. Contributions to an insect fauna of the amazon valley. Lepidoptera: Heliconidae. *Transactions of the Linnean Society of London*. 1862; 23, 495–566.
55. Razek A. Matching of an observed event and its virtual model in relation to smart theories, coupled models and supervision of complex procedures—A review. *Comptes Rendus Physique*. 2024; 25, 141–156.
56. Razek A. Strategies for managing models regarding environmental confidence and complexity involved in intelligent control of energy systems—A review. *Advances in Environment and Energies*. 2023; 2, aee020104.
57. Kou M, Dong X, Liu H, Zhou Q, Lin Q An adaptive multi-fidelity surrogate-based robust optimization approach considering the combined effect of various uncertainties *Engineering with Computers* 10.1007/s00366-025-02236-742:2 Online publication date: 26-Feb-2026 <https://dl.acm.org/doi/10.1007/s00366-025-02236-7>
58. Choubey S, Rahi S, Pal B, Agrawal M A novel data generation scheme for surrogate modelling with deep operator networks *Engineering Applications of Artificial Intelligence* 10.1016/j.engappai.2025.112086161:PA Online publication date: 1-Dec-2025 <https://dl.acm.org/doi/10.1016/j.engappai.2025.112086>.
59. Lebensztajn L, Marretto C.A.R, Caldora Costa M, Coulomb J.L. Kriging: A useful tool for electromagnetic device optimization. *IEEE Transactions on Magnetics*. 2004; 40, 1196–1199.
60. Gaignaire R, Scorretti R, Sabariego R.V, Geuzaine C. Stochastic uncertainty quantification of eddy currents in the human body by polynomial chaos decomposition. *IEEE Transactions on Magnetics*. 2012; 48, 451–454.
61. Den Boer J.A, Bourland J.D, Nyenhuis J.A, Ham C.L, Engels J.M, Hebrank F.X, Frese G, Schaefer D.J. Comparison of the threshold for peripheral nerve stimulation during gradient switching in whole body MR systems. *Journal of Magnetic Resonance Imaging*. 2002; 15, 520–525.
62. Davids M, Guerin B, Klein V, Wald L.L. Optimization of MRI Gradient Coils with Explicit Peripheral Nerve Stimulation Constraints. *IEEE Trans. Med. Imaging*. 2021; 40, 129–142.
63. Thylur D.S, Jacobs R.E, Go J.L, Toga A.W, Niparko J.K. Ultra-High-Field Magnetic Resonance Imaging of the Human Inner Ear at 11.7 Tesla. *Otology & Neurotology*. 2017; 38, 133–138.
64. Crozier S, Liu F. Numerical evaluation of the fields induced by body motion in or near high-field MRI scanners. *Progress in Biophysics and Molecular Biology*. 2005; 87, 267–278.
65. van Osch M.J.P, Webb A.G. Safety of Ultra-High Field MRI: What are the Specific Risks? *Current Radiology Reports*. 2014; 2, 61.
66. Bouisset N, Laakso I. Induced electric fields in MRI settings and electric vestibular stimulations: Same vestibular effects? *Experimental Brain Research*. 2024; 242, 2493–2507.
67. Mian O.S, Li Y, Antunes A, Glover P.M, Day B.L. On the Vertigo Due to Static Magnetic Fields. *PLoS ONE*. 2013; 8, e78748.
68. Boegle R, Dieterich M, Kirsch V. Comment on: Modulatory Effects of Magnetic Vestibular Stimulation on Resting-State Networks Can be Explained by Subject-Specific Orientation of Inner Ear Anatomy in the MR Static Magnetic Field. *Journal of Experimental Neurology*. 2020; 1, 109–114.
69. Li G, Patel N.A, Melzer A, Sharma K, Iordachita I, Cleary K. MRI-guided lumbar spinal injections with body-mounted robotic system: Cadaver studies. *Minim. Minimally Invasive Therapy & Allied Technologies*. 2022; 31, 297–305.

70. Yu N. Gassert R. Riener R. Mutual interferences and design principles for mechatronic devices in magnetic resonance imaging. *International Journal of Computer Assisted Radiology and Surgery*. 2011; 6, 473–488.
71. Zhou X. Wu S. Wang X. Wang Z. Zhu Q. Sun J. Huang P. Wang X. Huang W. Lu Q. Review on piezoelectric actuators: Materials, classifications, applications, and recent trends. *Frontiers in Mechanical Engineering*. 2024; 19, 6.
72. Okegbile S. D. Cai J. Zheng H, Chen J. Yi C. Differentially Private Federated Multi-Task Learning Framework for Enhancing Human-to-Virtual Connectivity in Human Digital Twin. *IEEE Journal on Selected Areas in Communications*. 2023; 41(11), 3533-3547.
73. Yang Y. et al. Dynamic Human Digital Twin Deployment at the Edge for Task Execution: A Two-Timescale Accuracy-Aware Online Optimization. *IEEE Transactions on Mobile Computing*. 2024; 23(12), 12262-12279.
74. Chen J. Yi C. Okegbile S. D. Cai J. Shen X. Networking Architecture and Key Supporting Technologies for Human Digital Twin in Personalized Healthcare: A Comprehensive Survey. *IEEE Communications Surveys & Tutorials*. 2024; 26(1), 706-746.
75. Chen J. Shi Y. Yi C. Du H. Kang J. Niyato D. Generative-AI-Driven Human Digital Twin in IoT Healthcare: A Comprehensive Survey. *IEEE Internet of Things Journal*. 2024; 11 (21), 34749-34773.
76. Razek, A.; Pichon, L. Smart Digital Environments for Monitoring Precision Medical Interventions and Wearable Observation and Assistance. *Technologies*. 2026; 14, 40.
77. Razek, A. Image-Guided Autonomous Robotic Surgery in the Context of Therapies Managed by Intelligent Digital Technologies: A Narrative Review. *Surgeries*. 2026; 7, 26.
78. Razek, A.; Bernard, Y. Potential of Piezoelectric Actuation and Sensing in High Reliability Precision Mechanisms and Their Applications in Medical Therapeutics. *Actuators*. 2025; 14, 528.